# Dynamics of photoinduced collisions of cold atoms probed with picosecond laser pulses

Fredrik Fatemi, Kevin M. Jones,[1] He Wang,[2] Ian Walmsley,[3] and Paul D. Lett
*Atomic Physics Division, National Institute of Standards and Technology, Gaithersburg, Maryland 20899-8424*
[1]*Department of Physics, Williams College, Williamstown, Massachusetts 01267*
[2]*Electronics and Photonics Laboratory, The Aerospace Corporation, El Segundo, California 90245*
[3]*Institute of Optics, University of Rochester, Rochester, New York 14627*
(Received 2 February 2001; published 17 August 2001)

Pump-probe experiments are performed in which cold colliding Na atoms are photoassociated to form $Na_2$ molecules, and subsequently ionized. The experiments are performed in a regime where the pulsed photoassociation to an intermediate potential takes place at long range, and to several electronic, vibrational, and rotational states. A probe pulse then produces an ionization signal by further exciting these molecules to autoionizing doubly excited states. The time dependence of the ion signal shows a dramatic flux-enhancement effect on a nanosecond time scale due to the motion on the intermediate potentials. This time dependence can be viewed as monitoring the inward motion and dephasing of a population wave packet formed at long range.

DOI: 10.1103/PhysRevA.64.033421 PACS number(s): 32.80.Pj, 34.20.Cf, 34.50.Rk, 34.80.Qb

A number of experiments in recent years have shown the way in which atomic and molecular dynamics can be illuminated using femtosecond laser pulses [1]. There has also been much written about the dynamics of ultracold collisions, in which the time scale of the relevant collision processes can become many nanoseconds [2–5], thus no longer requiring femtosecond resolution for study. Here we present experiments that begin to combine the pump-probe, pulsed-laser techniques originally developed for the study of fast molecular dynamics with the slow collisions of ultracold atoms in order to study the dynamics of a photoassociation-ionization process in sodium on the nanosecond time scale.

Proposals for experiments where wave packet motion might be probed in cold-atom collisions were discussed in the literature [6], but the only experiments reported were performed in a regime where the excitation can be considered as narrowband or cw [2–5]. Boesten *et al.* [4], for example, looked at the time dependence of a signal from a shape resonance in Rb photoassociation. In these experiments the photoassociating laser addresses a single rotational line of one vibrational state. While probing the evolution of the colliding atomic population, such an experiment does not create a coherent superposition of excited states required for wave-packet formation in the molecule.

The combination of ultracold photoassociation [7–9] and subsequent molecular ionization has been used with continuous-wave lasers to perform photoassociative-ionization spectroscopy [7,10–13]. In sodium two atoms in the $3S$ ground state collide, and are photoassociated to bound, excited molecular states by the absorption of a photon. The molecule can then be transferred to an autoionizing potential by the absorption of a second photon (see Fig. 1). The photoassociation step depends on there being a bound state available in the molecule, and is very frequency sensitive. The second step can take place to an ionization continuum just above the doubly excited asymptote [14]. This allows one to produce a spectrum of the excited diatomic molecules by measuring the ionization signal as a function of the photoassociating laser frequency with a fixed-frequency ionization laser. Alternatively, for the ionization step one can use a pulsed laser with a sufficient spectral width to access many autoionizing states near the dissociation limit, including bound states [15], to obtain such a spectrum.

In the present experiments we investigate the dynamics of the collision-ionization process by initiating the photoassociation using a short ($\approx$15 ps) pulse of light. Some of the molecules formed are subsequently ionized by a second, similar, laser pulse. The dynamics of the process can be investigated by varying the time delay between the two pulses. The bandwidths of the pulses are large enough that one can no longer treat the photoassociation process as if the light were from a narrow, cw laser. In this case the pulse spectrum is broad and many vibrational levels can be excited. If only a few states are excited the population cannot easily be localized on the potential. The formation of a spatially localized population wave packet requires the excitation of a superposition of $\approx$4 vibrational states, as indicated in Fig. 1(a). In the present experiments a relatively large number of vibrational states near the dissociation limit (binding energies

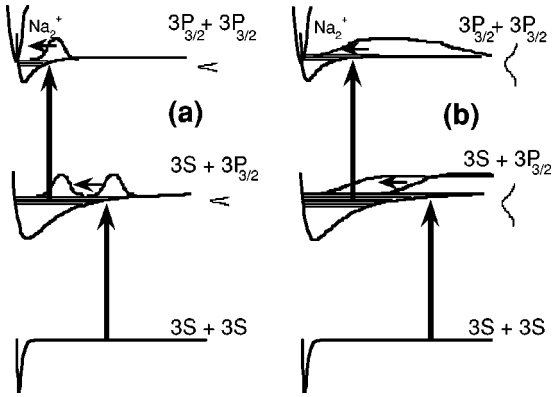


FIG. 1. Sketch of the potential energy for a pair of colliding atoms versus the internuclear distance, and bound energy levels involved in the experiment. The pulse frequency bandwidths, as indicated to the right of the potentials, overlap many rovibrational states. (a) Coherent wave-packet motion on the intermediate potential. (b) Simple spreading of the population on the intermediate potential, or dephasing of the broad population wave packet.

 

$<60$ GHz) are excited. This is because the photoassociation process is most efficient near the molecular dissociation limit, where the excited-state wave functions, weighted heavily toward the outer turning points, overlap well with the collisional wave functions. In this region the density of vibrational states in a $C_3R^{-3}$ potential becomes quite high (separations $\leqslant 5$ GHz), and the signals are strong enough to perform the experiments.

The population ''wave packet'' that is formed on the excited potential in this case is quite broad, and extends from moderate to large internuclear separations. The wave packet then spreads, fills in at short range, and decays. As the population moves slowly inward to shorter internuclear distances it can be probed with a second pulse of the same color light, which causes ionization through a doubly excited state [Fig. 1(b)]. The inverse of the local level spacing sets the time scale of any motion on the potential surface. In this case it indicates that the dephasing should take place on the time scale of about a nanosecond. The present one-color, pump-probe experiments do not resolve recurrences or other coherent wave-packet dynamics on the anharmonic intermediate-state potential, although there is hope that this might be accomplished in the future.

The motion of the population on the $S+P$ molecular potential results in an ionization signal from the second pulse which rises on a time scale of a few nanoseconds, as expected. Competing against this enhancement due to the motion is radiative decay of the population back to the $S+S$ potential. This occurs on a time scale related to the atomic lifetime, here 16 ns. In addition, flux enhancement effects of the type reported in Refs. [2,3] are observed. In those experiments a narrowband laser populated the $S+P$ potential at a specific internuclear distance, while in the present experiment the pulsed excitation will populate this potential over a broad range of (large) internuclear distances. The present experiments are a further illustration of the importance of the $R^{-3}$ long range interaction potential between ground and excited atoms, and how it can substantially modify the dynamics of ultracold collisions [16].

Although we have introduced a molecular picture of the experiment, it can also be described in terms of an atomic collision process. The first laser pulse creates a sample of excited atoms which can collide and undergo an associative ionization reaction. The second pulse creates more excited-state atoms, resulting in an increase in the ionization signal. We observe that the ion signal increases if the delay between the pulses is made to be several nanoseconds, and an understanding of this requires taking into account the ground-state–excited-state interaction. The strong attractive long-range interaction [16] between a pair of ground- and excited-state atoms causes such pairs to be drawn together in the time between the pulses. The second pulse converts such pairs into pairs of colliding excited-state atoms. The attractive interaction produces a strong enhancement in the number of such pairs which are able to survive to short range to autoionize and produce the signal.

We perform the experiments in a continuously-loaded dark spot magneto-optical trap (MOT) [17], and the setup is similar to that used in a number of previous experiments [7,18]. This leaves the atoms in the $F=1$ hyperfine state when the MOT light is turned off. Atoms are confined with temperatures of approximately 0.5 mK, and densities in the $10^{10}-10^{11}$-cm$^{-3}$ range. We detect the ions that are produced with a channel electron multiplier. The light pulses are obtained from a cavity-dumped, synch-pumped dye laser pumped with a mode-locked Nd:YAG (yttrium aluminum garnet) laser system with an 80-MHz repetition rate. The full 80-MHz repetition rate of the laser allows only $\approx 12$ ns between the pulses. This is unacceptable since the Na atomic lifetime is $\approx 16$ ns, and most of the molecular lifetimes we are concerned with are also in the range of 8–16 ns. Thus each pump pulse becomes a probe pulse for population left from the previous pump-probe pair if the repetition rate is this high. Consequently, we cavity dump the dye laser at a much lower rate to eliminate this problem. This also enables us to perform ion time-of-flight discrimination. Such a discrimination is important because of the high probability of producing atomic ions from other processes under some conditions, masking the signal.

The molecules are formed with very little kinetic energy (approximately the same as the $\approx 0.5$-mK temperature of the atoms they are formed from), and the ejection of an electron does not impart any significant momentum to the ion. Therefore, the time of flight to the detector is fixed for a given ion species. Previous experiments have shown that $Na_2^+$ ions can be photodissociated [19,20], and may arrive at the detector as $Na^+$ if this happens. This ionization process is not very efficient under conditions similar to those present here, however, and this is not expected to be a significant effect. In any event, this would only decrease our molecular ion signal. The fact that we see nearly 100% molecular ions under our experimental conditions confirms that photodissociation of $Na_2^+$ is not important. The molecular ions in our particular apparatus require approximately 2.3 $\mu$s to arrive at the detector. Given the cold, essentially point source of ions, the factor of 2 mass difference in the species gives a $\sqrt{2}$ difference in the flight time, and we can easily distinguish them. The experiments were performed with a 300-kHz repetition rate, allowing 3.33 $\mu$s between the pulses. A clear sorting of the ions by mass was then made by using 300-ns counting windows centered on the mean arrival times. The MOT is operated with a 50% duty cycle $-100$ $\mu$s on followed by 100 $\mu$s off. The pulsed laser is introduced continuously; however, the ions that are created during the MOT-on phase of the trap are discarded, and only those created when the MOT light is off are gated into the counters.

A sufficiently low intensity ($<10$-kW/cm$^2$ or $<100$-$\mu$W average power at a 300-kHz repetition rate, in a spot of 500 $\mu$m radius) makes it possible to produce molecular ions almost exclusively. The signal remaining in the atomic ion channel is consistent with detector noise. At higher intensities the ions become predominantly $Na^+$ atomic ions produced by three-photon ionization of the atoms, instead of the desired two-photon photoassociation and ionization of molecules. (Absolute intensities given here are uncertain to a factor of 5 due to difficulties in measuring the beam diameter at the position of the MOT.) Typical signal rates were approximately one count per $10^4$ laser pulses or less.

The dye laser pulses are approximately 15 ps in duration, leading to a 60-GHz bandwidth. The pulses are tuned so that their bandwidth overlaps the $3S$-$3P_{3/2}$ atomic transition. The experimental results are not qualitatively very different over the entire range of detunings where we were able to obtain data. In fact, even quantitatively we were unable to vary the time scales by any significant or discernable amount over the range where we still were able to obtain a signal. To obtain a usable signal the laser is tuned so that the pulse spectrum is typically centered $10\pm10$ GHz below the $S+P_{3/2}$ dissociation limit. This tuning produced the best signals, although larger detunings and detunings of the center frequency above the dissociation limit produced similar, athough smaller, signals. In short, over the limited range of detunings available to us, which required the laser spectrum to overlap the dissociation limit, the signal was not qualitatively sensitive to detuning.

Each pulse is split to form pump and probe pulses $P_1$ and $P_2$, which can be autocorrelated in a nonlinear KDP crystal or sent to interact with the atoms in the MOT at times $T_1$ and $T_2$, respectively. The light in the two pulses is parallel and linearly polarized. The pulse spectrum is monitored with a grating spectrometer, and adjusted to be smooth and close to transform limited. For the data presented here the pulse spectrum is nominally centered on the atomic transition. The pulse delay $\Delta T=T_1-T_2$ is tunable from $-15$ to $+15$ ns by a computer-driven delay line. Large beam diameters were used for low divergence, so as to maintain good beam overlap over the large distances implied by these delays. The beams are recombined on a nonpolarizing beam splitter. At high intensities three-photon ionization of Na atoms produces an atomic autocorrelation signal that can be used to ensure good pulse overlap in the MOT for short delay times. Integrated counting periods of several seconds at each $\Delta T$ are used to measure both the $Na^+$ and the $Na_2{}^+$ signals under conditions with both pulses $P_1$ and $P_2$ entering the trap chamber, with only $P_1$ entering and $P_2$ blocked, and with $P_1$ blocked and $P_2$ entering.

Figures 2 and 3 show the molecular ion signal as a function of the delay $\Delta T$ out to 12 ns. From these figures, we can clearly identify three time scales on which the $Na_2{}^+$ ion signal exhibits different behaviors. For extremely short time scales, on the order of the pulse length ($\Delta T\leqslant 20$ ps), the signal exhibits a small ($\approx 10\%$) peak above the baseline signal (see Fig. 2). For 20 ps $<\Delta T<3$ ns, we observe a rapid rise in the signal [Fig. 3(a)], while for $\Delta T>4$ ns the signal decays gradually [Fig. 3(b)].

Even at low intensities a single pulse is able to produce molecular ions. This results from a two-photon resonant excitation of colliding atom pairs at long enough range to be resonant with the $S+P$ states within the bandwidth of the pulse. The pairs are excited to bound or continuum autoionizing states near the $P_{3/2}+P_{3/2}$ asymptote (see Fig. 1). The excited population must then travel on these weakly attractive ($V\propto C_5R^{-5}$) doubly excited potentials to small internuclear distances where autoionization can occur ($R<10a_0$). The probability that this occurs before radiative decay of the molecule is small because of the relative flatness of these potentials. Such survival factors are characteristic of cold collisions, as discussed in Refs. [21,22].

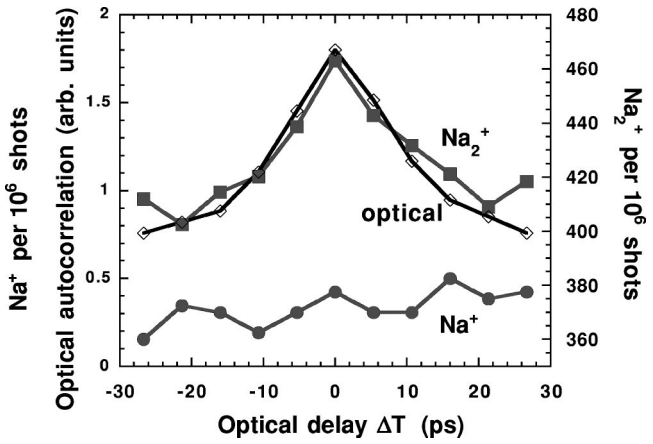


FIG. 2. Autocorrelation signal of the two pulses as measured by the $Na_2{}^+$ signal (filled squares) and the optical signals from a KDP crystal (open diamonds) as a function of the pulse delay time $\Delta T$. The $Na^+$ signal (filled circles) measured concurrently with the $Na_2{}^+$ signal is also shown. Note the large offset and different scale of the $Na_2{}^+$ signal.

The small time-dependent signal at the shortest time delays is an autocorrelation of the two laser pulses as seen in the molecular ion signal. Figure 2 compares the short-time dependence of the molecular ion signal with the optical autocorrelation signal obtained from overlapping the pulses in a KDP crystal. Clearly the shapes of the two signals agree quite well over the displayed range of times. If the direct two-photon $S+S\rightarrow P+P$ excitation process in the molecule were not nearly resonant with an intermediate state at long range, we could expect only this autocorrelation signal. The autocorrelation is due to the $I^2$ dependence of the excitation, as the temporal overlap of the pulses is varied. The existence of the intermediate $(S+P)$ state in the molecule causes the ion autocorrelation signal not to decay to a flat background when the pulses do not overlap, however. Thus the autocorrelation only decays by about 10% from its peak value.

We carried out a calculation of the expected autocorrelation signal, given the resonant intermediate state, the random phases of the electric fields of the pulses, and a 15-ps Gaussian pulse with a maximum intensity of 7 kW/cm$^2$ and a pulse area of 0.25. The calculation of the population of the upper level of a three-level system [23] given these fields gives a reasonable match to the 10% peak in the data. For this calculation of the short-time autocorrelation we ignore any nuclear motion. As can be seen in Fig. 3(a), the molecular autocorrelation signal at $\Delta T=0$ is less than the level that one would expect from adding the fields of the original pulses coherently [$\approx 440$ molecules/$10^6$ pulses in Fig. 3(a)], as it must be given the uncontrolled relative phases of the pulses. At these intensities the $Na^+$ atomic ionization signal is completely flat, and what little ionization we see in this channel is consistent with noise ($\leqslant 0.5$ counts/$10^6$ pulses). At higher intensities a clear autocorrelation signal can be seen in the $Na^+$ ion signal due to three-photon ionization of the atoms.

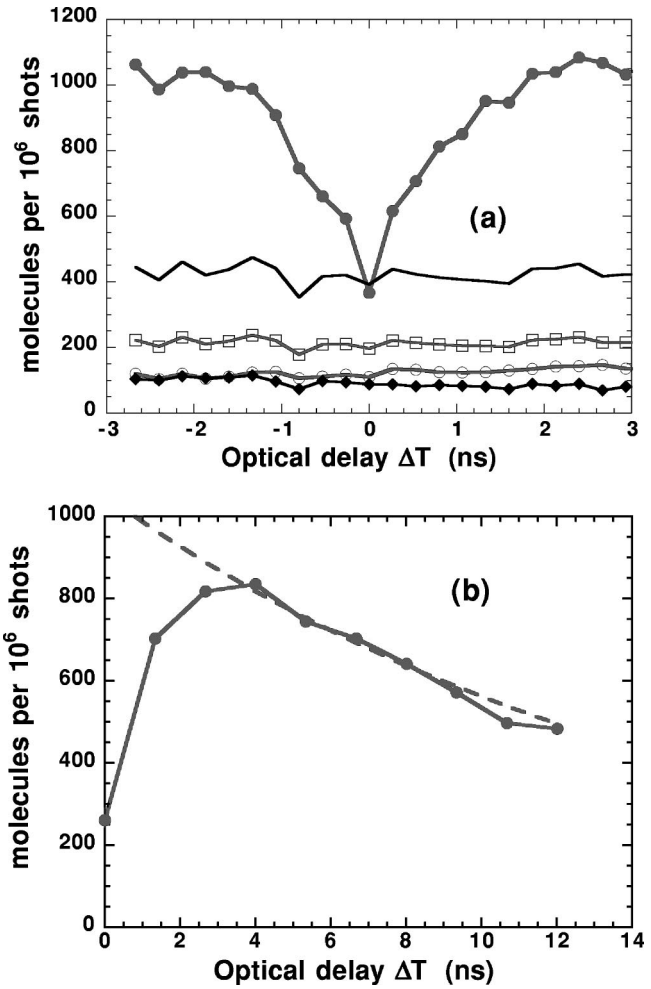


FIG. 3. Molecular ion signal versus optical delay $\Delta T$. The upper panel shows the signal on a time scale of $-3$ to $+3$ ns, while the lower panel shows the long time behavior out to 12 ns. In the upper panel the traces, from bottom to top, are the signals obtained as the optical delay is varied with only pulse $P_1$ entering the chamber, with only a pulse $P_2$ entering the chamber, the sum of these two signals, the ''coherent sum'' of the two pulses (the sum of the square roots of the signals, squared) and finally, the signal obtained with both pulses present. The ratio of the intensity in the pulse $P_1$ to that in pulse $P_2$ was measured to be 1.1:1, and the peak intensities were both approximately 10 kW/cm$^2$. In the lower panel the dashed line indicates an exponential decay with a 16-ns time constant for comparison with the data at large $\Delta T$. The laser detunings and the MOT density were slightly different when the data for the two plots was taken, leading to the differences in the signals.

On longer time scales, we begin to see a time dependence due to the dynamics of the colliding atoms. The $Na_2^+$ signal rapidly rises, reaching a maximum at $\Delta T \approx 3-4$ ns, and then slowly decays. The decay is approximately exponential in form, and has a decay constant of $\approx 16$ ns. During the 15 ps of the pulse, the pump laser excites some population to the relatively flat, doubly excited $P+P$ potential, as discussed above. In addition, it excites a much larger population to the potentials near the $S+P$, singly excited asymptote. These potentials have a steeply attractive, $C_3R^{-3}$ form, which rapidly accelerates the atoms toward one another. Subsequently, the probe pulse is also able to excite some small population from the ground $S+S$ state directly to the $P+P$ state, and take additional population from the ground state to the $S+P$ state. More importantly, however, it is able to take some of the population that has been placed on the $S+P$ potential by the pump pulse and promote it to the $P+P$ potential. This population has been accelerated on the attractive potential, and has moved to closer distances during the delay time between the pulses. This population, because of its higher velocity, has a much better probability of surviving on the $P+P$ potential to distances where autoionization can occur before it is removed by spontaneous emission. If the delay between the pulses is too long, however, the population will decay from the $S+P$ potential (lifetimes $\approx 12$ ns for a typical $Na_2$ molecular potential in this region), and the signal is again attenuated by poor survival. Between these two extremes excitation to the molecular $S+P$ potential allows approximately a threefold enhancement in the autoionization signal.

Another aspect of this signal enhancement is that, by going through the attractive $S+P$ states, we can overcome the angular momentum barriers that inhibit the higher partial waves from interacting on the $S+S$ and $P+P$ potentials. This analysis is similar to that given for the flux enhancement effects observed by others in ultracold systems [2,3]. By including higher partial waves, a much larger fraction of the phase space of atoms is available to contribute to the signal.

The delay-dependent signal of Fig. 3(b) should depend on the center frequency of the spectrum of the pulsed laser. We find that the more spectral power that is near the atomic resonance, the stronger the signal. The signal becomes smaller as the pulse spectrum is detuned below and away from resonance. This is both because the Franck-Condon factors for the photoassociation step go down and because the overlap with good ionization states in the second step becomes smaller. Unfortunately, there seems to be only a rather small detuning range where a reasonable signal is obtained. When we detuned far enough red that a single pulse did not produce a molecular ion signal, we also found no pump-probe signal. Before reaching that point the pump-probe signal remained similar in form but became smaller at larger detunings. From additional experiments comparing cw photoassociation with pulsed ionization and pulsed photoassociation with cw ionization, it is apparent that the poor efficiency of pulsed photoassociation is the limiting factor in these experiments.

We have modeled the system (for nonoverlapping pulse delays) using a simple classical Monte Carlo simulation of the atom-pair trajectories. Although the simulation is based on a vast simplification of the actual physical system, it reproduces most of the experimental features reasonably well. There are several potentials that might be involved at both the $S+P$ and $P+P$ asymptotes. Nevertheless, we abstract these to a single potential at each of the asymptotes, and give these representative potentials some average properties characteristic of the sodium dimer.

The initial ensemble is assumed to be of uniform density in three dimensions, so that the probability of finding two

atoms separated by a distance $R$ scales as $R^2$. $R$ is allowed to vary over a range of $0a_0$ to $2000a_0$ ($1a_0=0.0529177$ nm). Each atom is given a velocity from a Maxwell-Boltzmann distribution corresponding to a 500-$\mu$K temperature. An atom and its collision partner are selected, and the relative approach velocity and classical angular momentum of the pair are recorded. The atoms are then allowed to propagate on a set of one-dimensional potentials in the internuclear coordinate $R$, including the appropriate angular momentum barriers.

We assume for simplicity that the excitation probability is independent of the internuclear separation (dipole moment independent of $R$), which approximately holds over the separations involved [24]. The initial distribution naturally weights the excitation toward large internuclear separations, where most of the population is. At $T=0$, the atoms are excited and placed onto the $C_3R^{-3}$, $S+P$ potential, where they accelerate toward small $R$. The system is allowed to evolve for a time $\Delta T$ on this potential. During this time the population is reduced by a survival factor to account for spontaneous decay. The factor is given by the molecular state lifetime that corresponds to the value of $C_3$. At the time of the second pulse the population from the $S+P$ potential is moved to, and allowed to travel on, an attractive $C_5R^{-5}$, $P+P$ potential. This population is again allowed to decay with an exponential lifetime characteristic of this state, and any population surviving in to a separation of $30a_0$ is considered to have ionized and is counted as signal. The additional time to reach $R=0$ from $30a_0$ is at most 6 ps for any reasonable choice of $C_5$, which is negligible compared to the lifetime of the state.

The states that are asymptotically $S+P_{3/2}$ are well known from cw spectroscopy [18], with $1_g$, $0_g^-$, and $0_u^+$ symmetries. The potentials near the $P+P$ asymptote are not as well characterized [15]. The present experiments may very well involve several potentials at each asymptote. It is impossible to tell, however, which of these may be contributing. Since the potentials at both the $S+P$ and $P+P$ asymptotes are neither identified nor selected for, the $C_3$ and $C_5$ coefficients are chosen to have more or less ''average'' values for $Na_2$ potentials. $C_3=-10.0$ a.u. is taken as an average or''typical'' value [24], corresponding to a lifetime of $\approx 12$ ns. (The atomic units for $C_3$ are hartree $a_0^3$; 1 hartree$=4.359\times10^{-18}$ J.) Recent experiments examining the pathways to cw photoassociative ionization [15,25] have shown that $0_u^-$ and $1_u$ doubly excited states with $C_5$ values of approximately $-250$ a.u. (atomic units for $C_5$ are hartree $a_0^5$) are major contributors. We use a value of $C_5=-250.0$ a.u. and a lifetime of 8 ns for this state in the model.

The results from the simulations are shown in Fig. 4, along with the data. Although experimentally we observe that a single pulse can excite population directly to the $P+P$ potential, there is no provision for this in the simulation. In the absence of depletion of the ground-state population, this should only result in a constant offset to the signal. We did not use an offset in Fig. 4. The overall height of the simulated signal is adjusted to match the data.

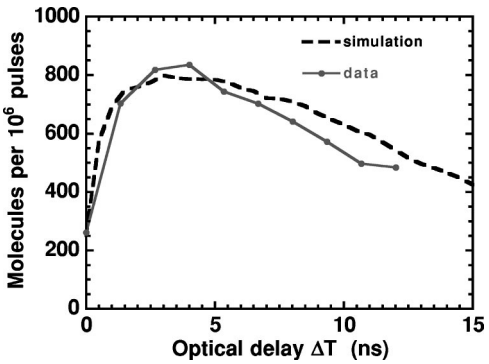


FIG. 4. Number of molecular ions collected per $10^6$ pulse pairs versus the optical delay $\Delta T$. Experimental results (solid points with a line to guide the eye) are compared with the simulation results (dashed line).

The scatter in the data gives a representation of the reproducibility and statistical uncertainty in the data. The scatter is a bit worse than purely statistical [as can be seen in Fig. 3(a)]. This is mostly due to the fluctuations in the MOT laser intensity and frequency, which result in fluctuations in the density of trapped atoms. Some variation in the detuning of the pulsed laser from day to day also contributes to the uncertainty in our signal size. The important results of the experiment are qualitative. We can see a time-delay dependence of the signal, with a peak signal that is a factor of 3 or 4 larger than that at very short delays, and it appears at a delay of $3.5\pm1$ ns. The uncertainty in our measurements is such that we cannot determine the height of this peak to better than about 25%. That the peak occurs on a time scale of several nanoseconds is also important. It identifies it as a dynamical effect; we can clearly distinguish it from processes on much faster or slower time scales, such as the pulse autocorrelation and the long-time decay of the signal due to spontaneous emission.

The important features seen in the data are reproduced by the simulations. In particular, the signal rises from short delay times to peak near 3–4-ns delay. The signal then decays with a time constant of about 16 ns. (The decay is not necessarily exponential, and it does not simply derive from the 16-ns atomic lifetime; while obviously related to it, this number is not explicitly present in the simulations.) The offset or zero-delay signal in the simulation comes from the first pulse exciting population to the $S+P$ state and the second pulse placing this population on the $P+P$ state without allowing any propagation on the $S+P$ potential. The short-time autocorrelation is explicitly not included in the model.

The simulations allow one to examine where the signal originates from for different delay times, information not available in the experiment. Figure 5(a) shows the population that contributes to the signal as a function of the starting internuclear separation, for different delay times. It is easy to see both the effect of the expanding phase space and the increased survival factor due to travel on the intermediate potential. At increasing delay times atom pairs at larger internuclear separations contribute to the signal; the pairs that are excited at long range can approach on the intermediate $S+P$ potential, and gain enough velocity to survive to short

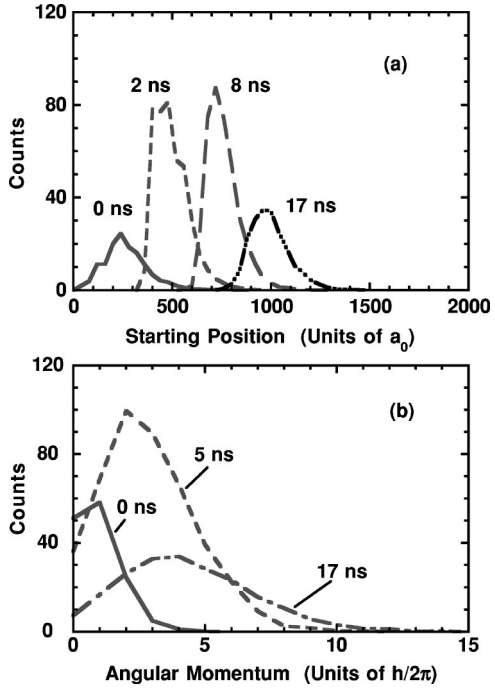


FIG. 5. Simulation results. (a) The relative contributions to the signal of different initial internuclear separations for pulse delay times of 0, 2, 8, and 17 ns. (b) The relative contribution to the signal of different angular momentum partial waves for pulse delay times of 0, 5, and 17 ns.

range and contribute to the signal. The fact that there are more and more pairs available in the expanding $R^2dR$ shell allows the signal to grow for longer delays. Radiative decay from both the $S+P$ and the $P+P$ potentials causes population starting from $1000a_0$ or further out to be severely attenuated; even the $R^{-3}$ potential is quite flat at these distances, and the population takes too long to approach the $30a_0$ cutoff that represents ionization. At very short delay times the population that is excited at long range (where most of the pairs are) must travel most of the distance to short range on the $R^{-5}$, $P+P$ potential with a small velocity. Again, decay from spending a long time on this flat potential supresses the signal. The difference between travel on the $R^{-3}$ and $R^{-5}$ potentials can be seen by comparing how far an atom, initially at rest, can travel in 20 ns on each potential. Pairs placed on the $C_3R^{-3}$ potential ($C_3=-10$ a.u.) will travel from $1000a_0$ to $50a_0$ in this time, while on the $C_5R^{-5}$ potential ($C_5=-250$ a.u.) only population from $R<500a_0$ will arrive. In fact, the $C_3$ potential dominates the dynamics for all but the shortest delay times and setting $C_5 = 0$ in the simulation (a flat doubly excited potential) makes very little difference. The peak in the signal near a delay of 3–4 ns can be modified somewhat by changing the value of the $C_3$ coefficent, while only the behavior near $\Delta T=0$ is affected by the value of the $C_5$ coefficient.

In the simulations we can also examine the contributions to the signal of the various angular momentum partial waves for different $\Delta T$, as seen in Fig. 5(b). At short delay times only the lowest partial waves can contribute to the signal; primarily $s$ and $p$ waves, and limited to $l\leqslant 3$. For a delay of 5 ns the distribution of partial waves peaks around $l=2$, and cuts off around $l=7$ or 8. For delays as long as 17 ns the contributions to the signal peak around $l=4$, and cut off around $l=9$ or 10. The contribution of these higher partial waves helps increase the signal size at longer delays. Population accelerating in on the $S+P$ potential can get past the angular momentum barriers that exist to a much greater extent on both the $S+S$ and $P+P$ potentials. It can then be promoted to the $P+P$ potential inside of these barriers.

Our classical discussion of the motion on the internuclear potentials of the quasi molecule and survival on these potentials is very similar to that given by Gallagher and Pritchard [22] early in the investigation of ultracold collisions. Although that model has been used to describe some trap loss experiments, it is not directly applicable to cw photoassociation. In the short pulse regime explored in the present experiment the discrete level spacing of the molecule is not important and such a classical description is acceptable.

The present experiments are similar in spirit to many femtosecond pump-probe experiments that demonstrate wave-packet dynamics on molecular potentials. The ''wave packet'' that is created in the present experiments, however, is not one that could demonstrate the recurrences suggested in Ref. [6]. The population on the intermediate-state potential is in a superposition of so many vibrational levels that the rather extended wave packet that is excited by the pump pulse simply ''dephases,'' and the population diffuses toward short range, as in Fig. 1(b), rather than moving as a localized wave packet, as indicated in Fig. 1(a). The signal rises as this wave packet fills in at short range, and then decays as the (now fully diffuse and dephased) wave packet decays.

In order to study coherent wave-packet motion experimentally a larger detuning, where the laser bandwith covers only 4–5 vibrational states, is required [Fig. 1(a)]. In that situation, however, no ionization signals were observed in our apparatus. In the future such experiments may be possible, but they will require a more efficient path to ionization than available here using a single color. Using pump and probe pulses with different central frequencies may allow the excitation pulse to be detuned so as to excite only a limited number of vibrational states. At the same time the probe can then be tuned to optimize the ionization probability from these particular states.

Pulsed-laser experiments such as these can sometimes help reveal the dynamics behind the similar cw experiments. In the present case the two-photon, single-color cw photoassociation or ionization process can apparently take place via several pathways (excitation to doubly excited autoionizing states as well as short-range direct excitation to the molecuar ion [19]), but it is not clear that these channels are the same ones that are open in the case of pulsed excitation. The fact that the behavior of the signal size as a function of detuning is different in the two cases suggests that, at least under these conditions, they are not.

Machholm *et al.* in Ref. [6] did not consider pulse detunings such that the probe pulse could produce excitation above the $P_{3/2}+P_{3/2}$ asymptote. In the detuning regimes they considered these authors suggested that a large contribution

to the ionization results from excitation of the population on the $S+P_{3/2}$ intermediate potentials to ionization continua above the $P_{1/2}+P_{1/2}$ or $P_{1/2}+P_{3/2}$ asymptotes. In the present experiments these channels should be open, although no evidence of ionization through them is seen. If the detuning of the lasers in the experiment is such that the bandwidth of the pulse does not allow excitation above the $P_{3/2}+P_{3/2}$ asymptote, the ionization signal disappears. On the other hand, it may once again be a function of the poor photoassociation efficiency that we cannot see evidence of this channel. Two-color cw photoassociation experiments did produce evidence of ionization 1 mK above the $P_{1/2}+P_{3/2}$ asymptote [14], but the weakness of the signal indicated that there may be a barrier to ionization on this potential. Presumably here the excitation (near the $P_{3/2}+P_{3/2}$ asymptote and $\approx 17$ cm$^{-1}$ above the $P_{1/2}+P_{3/2}$ asymptote) would be above any very weak barrier. Nevertheless, a barrier of 17 cm$^{-1}$ or more, of course, would still explain the present results.

An interesting future step in pulsed-laser photoassociation experiments will be the study of a pulsed-Raman STIRAP (stimulated Raman adiabatic passage, or counter intuitive pulse order) type of excitation [26–28]. In particular the desire to form stable bound ground states of cold dimer molecules drives this interest. Recently there has been some controversy in the literature about pulsed photoassociation rates in the form of a question as to whether STIRAP-type excitation will work at all in a MOT, and whether the rates will be enhanced in the situation of photoassociation in a Bose-Einstein condensate [27,28]. The intensities required for adiabatic passage with pulse durations on the order of 10 ps makes such experiments unrealistic, as the present results indicate that atomic ionization would dominate. On the other hand, longer pulses may still be effective, and such investigations are planned.

While the broad bandwidth of femtosecond pulses makes them ideal for spectral manipulation, the slow time scales in cold-atom experiments may make them well suited for manipulation by temporal shaping of pulses. We can hope that in the future these kinds of experiments will lead to a variety of coherent control with time-dependent pulses that will enable the experimenter to guide the dynamics of the slow photoassociation collisions, rather than just observe them.

We would like to thank Michael Casassa and Ted Heilweil for the loan of the pulsed YAG laser system and assistance in getting it working. We would also like to thank a number of people for their input over the years since the inception of the idea: Vanderlei Bagnato, Nick Bigelow, Marya Doery, Paul Julienne, Paul Leo, Mette Machholm, Seyffie Maleki, Luis Marcassa, Fred Mies, Annick Suzor-Weiner, Eite Tiesinga, John Weiner, and Carl Williams.

[1] See, for example, L.R. Khundkar and A.H. Zewail, Annu. Rev. Phys. Chem. **41**, 15 (1990); A.H. Zewail, Faraday Discuss. Chem. Soc. **91**, 207 (1991); T. Baumert, M. Grosser, R. Thalweiser, and G. Gerber, Phys. Rev. Lett. **67**, 3753 (1991).
[2] S.D. Gensemer and P.L. Gould, Phys. Rev. Lett. **80**, 936 (1998).
[3] C. Orzel, S.D. Bergeson, S. Kulin, and S.L. Rolston, Phys. Rev. Lett. **80**, 5093 (1998).
[4] H. Boesten, C. Tsai, B. Verhaar, and D. Heinzen, Phys. Rev. Lett. **77**, 5194 (1996); H. Boesten, C. Tsai, D. Heinzen, A. Moonen, and B. Verhaar, J. Phys. B **32**, 287 (1999).
[5] H. Boesten, C. Tsai, D. Heinzen, A. Moonen, and B. Verhaar, J. Phys. B **32**, 287 (1999).
[6] M. Machholm, A. Guisti-Suzor, and F. Mies, Phys. Rev. A **50**, 5025 (1994).
[7] P.D. Lett, P.S. Julienne, and W.D. Phillips, Annu. Rev. Phys. Chem. **46**, 423 (1995).
[8] D.J. Heinzen, in *Atomic Physics 14*, edited by D. Wineland, C. Wieman, and S. Smith (AIP Press, New York, 1995), p. 369.
[9] J. Weiner, V.S. Bagnato, S. Zilio, and P.S. Julienne, Rev. Mod. Phys. **71**, 1 (1999).
[10] P.D. Lett, L.P. Ratliff, M.E. Wagshul, S.L. Rolston, and W.D. Phillips, in *Resonance in Ionization Spectroscopy 1994*, edited by H.-J. Kluge, J. E. Parks, and K. Wendt, AIP Conf. Proc. No. 329 (AIP, New York, 1995), p. 289.
[11] P.A. Molenaar, P. van der Straten, and H.G.M. Heideman, Phys. Rev. Lett. **77**, 1460 (1996).
[12] H. Wang, X.T. Wang, P.L. Gould, and W.C. Stwalley, Phys. Rev. Lett. **78**, 4173 (1997).
[13] J.P. Shaffer, W. Chalupczak, and N.P. Bigelow, Phys. Rev. Lett. **82**, 1124 (1999); **83**, 3621 (1999).
[14] K.M. Jones, S. Maleki, L.P. Ratliff, and P.D. Lett, J. Phys. B **30**, 289 (1997).
[15] A. Amelink, K.M. Jones, P.D. Lett, P. van der Straten, and H.G.M. Heideman, Phys. Rev. A **61**, 042707 (2000).
[16] A. Fioretti, D. Comparat, C. Drag, T. Gallagher, and P. Pillet, Phys. Rev. Lett. **82**, 1839 (1999).
[17] W. Ketterle, K.B. Davis, M.A. Joffe, A. Martin, and D. Pritchard, Phys. Rev. Lett. **70**, 2253 (1993).
[18] L.P. Ratliff, M.E. Wagshul, P.D. Lett, S.L. Rolston, and W.D. Phillips, J. Chem. Phys. **101**, 2638 (1994).
[19] J.J. Blangé, J.M. Zijlstra, A. Amelink, X. Urbain, H. Rudolph, P. van der Straten, H.C.W. Beijerinck, and H.G.M. Heideman, Phys. Rev. Lett. **78**, 3089 (1997); J.J. Blang, X. Urbain, H. Rudolph, H.A. Dijkerman, H.C.W. Beijerinck, and H.G.M. Heideman, J. Phys. B **29**, 2763 (1996); **30**, 565 (1997).
[20] V. Bagnato (private communication).
[21] P. Julienne and F. Mies, J. Opt. Soc. Am. B **6**, 2257 (1989).
[22] A. Gallagher and D. Pritchard, Phys. Rev. Lett. **63**, 957 (1989).
[23] R. Brewer and E. Hahn, Phys. Rev. A **11**, 1641 (1975).
[24] P.S. Julienne and J. Vigue, Phys. Rev. A **44**, 4464 (1991).
[25] A. Amelink, K.M. Jones, P.D. Lett, P. van der Straten, and H.G.M. Heideman, Phys. Rev. A **62**, 013408 (2000).
[26] P.S. Julienne, K. Burnett, Y.B. Band, and W.C. Stwalley, Phys. Rev. A **58**, 797 (1998).
[27] A. Vardi, D. Abrashkevich, E. Frishman, and M. Shapiro, J. Chem. Phys. **107**, 6166 (1997).
[28] J. Javanainen and M. Mackie, Phys. Rev. A **58**, 789 (1998); M. Mackie, R. Kowalski, and J. Javanainen, Phys. Rev. Lett. **84**, 3803 (2000).